

Marián Činčala – Ludvík Kunz *

HIGH-CYCLE FATIGUE BEHAVIOUR OF 14 109 BEARING STEEL

Fatigue lifetime of 14 109 bearing steel in a high-cycle region in tension-compression has been studied experimentally. The aim was to determine the $S-N$ curve including fatigue limit, to perform fractographic observation and to analyze crack initiation sites, to discuss the large scatter of lifetime data, which is inherent to high strength steels, and to check the empirical $\sqrt{\text{area}}$ method to predict fatigue limit for this type of steel.

1. Introduction

Bearings are important machine parts, which have to sustain an extremely high number of loading cycles during their lifetime. Severe material and technological requirements are posed on the manufacturing of particular bearing parts. Structural steel 14 109, which has frequently been used for bearing bodies, balls and cylindrical roller bearings, fulfills these requirements. This steel is an equivalent of the European 100Cr steel, US E52100 through-hardening steel or Japanese SUJ2 and SUJ4 steels. The characteristic feature is higher content of C and Cr, which is an important prerequisite for superior mechanical properties. In spite of the fact that this steel belongs to the group of common structural steels, it still attracts research attention from the point of view of the relation among microstructure, mechanical properties and machining technology [1].

Extremely high fatigue lifetime is a crucial requirement for all types of bearing steels. Fatigue properties of high strength steels generally strongly depend on the surface state and on structural defects [2-3]. High quality clean steels, free from nonmetallic inclusions or other stress raisers are the primary requirement to achieve extended fatigue life. This holds above all in the high-cycle and giga-cycle fatigue regions. Defects on the surface – small notches, scratches, impressions and roughness – play an important role in the pitting process. However, suitable technological and production processes can eliminate them successfully. High quality finished surfaces, application of suitable lubricants diminishing friction and heat generation at contact areas significantly suppress this problem. On the other hand, details of microstructure and micro-purity remain important phenomena which determine the fatigue crack initiation and hence the fatigue lifetime. Irregularly distributed small carbides and non-metallic inclusions are the result of desoxidation process and of heat treatment. They often represent severe stress raisers. Fatigue cracks initiate predominantly in their vicinity. Whereas in the case of surface initiation the crack location and propagation can be monitored and described during the cyclic loading, in the case of internal initiation and crack propagation some open questions remain.

Fatigue lifetime data in high-cycle and giga-cycle region have been shown to exhibit a “two-stage” or “stepwise” $S-N$ curve, eg. [4-5]. Japanese researchers have performed the majority of these observations on bearing steels [6-10] using rotating bending fatigue machines. The main reason for the two-stage $S-N$ curve seems to be the transition from the surface to internal crack initiation in the very-high-cycle region. The discontinuity on $S-N$ curves and the change of the crack initiation from the surface to the interior has been usually reported in the interval between 10^6 to 10^7 cycles. Recently Marines et al. [11] have compared the S-N curves of bearing steel NF 1006C at frequencies of 35 and 30 kHz in tension-compression and in rotating bending. They indicate that the two-stage S-N curve is connected with the rotating bending; if the tension-compression loading is used, a continuously decreasing lifetime with decreasing stress amplitude is observed up to the giga-cycle region. Further, the fatigue limit of bearing steels defined between 10^6 to 10^7 cycles cannot guarantee a safe design.

The aim of this work was to experimentally determine the fatigue lifetime of bearing steel 14 109 in tension-compression and to analyze the crack initiation in the range of 10^6 to 10^7 cycles.

2. Material and experiments

Hypereutectic steel 14 109 with the chemical composition as given in Tab.1 has been used. The composition corresponds to that of E52100 and SUJ 2 steels.

Chemical composition of 14 109 steel (wt.%). Tab. 1.

C	Mn	Si	Cr	Ni	Cu	Ni+Cu	P	S
1.0	0.34	0.28	1.48	0.1	0.12	0.22	0.01	0.01

Button-end specimens for fatigue tests, Fig. 1, were prepared by cutting operation. The minimum gauge length diameter was machined with working allowance of 0.8 mm. Heat treatment consisted of austenitization at 1113 K for 20 min. followed by rapid

* Marián Činčala¹, Ludvík Kunz²

¹ Žilinská univerzita v Žiline, Veľký diel, 010 26 Žilina, Slovenská republika

² Ústav fyziky materiálu AV ČR, Žižkova 22, 616 62 Brno, Česká republika

quenching into oil (JS4). The resulting martensitic microstructure was annealed for stress relieving at 443 K with holding time of 90 min followed by air-cooling. The resulting microstructure consists of tempered martensite with regularly distributed carbides and residual austenite content of 6.35 ± 0.94 wt. % (determined by diffractometric analysis). The microstructure of heat-treated steel is shown in Fig.2. The hardness measured on the specimen cross-section varies between $650 \div 713$ HV and is well compared with the hardness reported in [11]. The gauge length with working allowance of 0.8 mm of heat-treated specimens was finely ground to the final diameter of 3 mm with the aim of removing the notch influence of the surface after cutting operation and of removing the decarburized layer. The final operation consisted of fine grinding by means of metallographic emery papers on a turn bench.

Fatigue tests were accomplished on resonant fatigue machine Amsler in controlled load. The cycling was characterized by sine load wave with frequency 190 Hz. The stress ratio R was equal to -1 . Experiments were performed at room temperature in the ambient air atmosphere. In the stress amplitude interval used, no heating of specimens was observed.

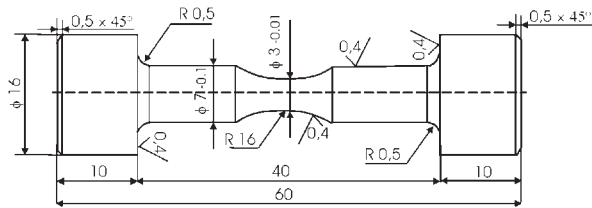


Fig. 1. Specimen for experimental determination of S-N curves.

3. Results

Experimentally determined lifetime of specimens loaded in tension-compression is shown in Fig. 3. The experimental data exhibit a considerable scatter. The highest stress amplitude at which

the run-out specimen (on the basis of 10^7 cycles) was found is 840 MPa.

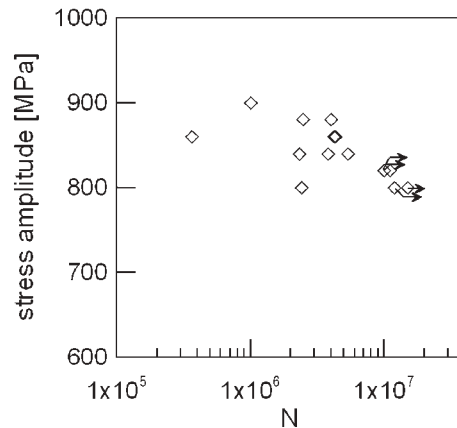


Fig. 3. S-N curve of 14 109 bearing steel.

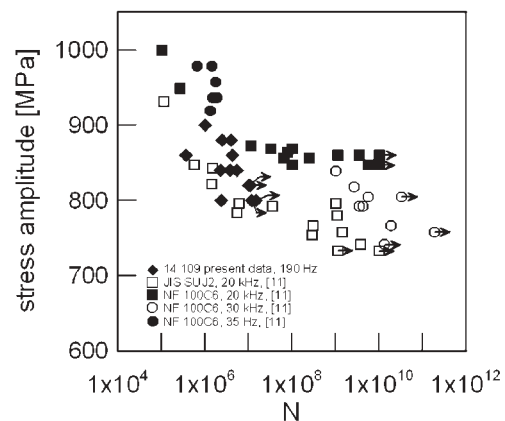


Fig. 6. Comparison of present results with literature data [11]

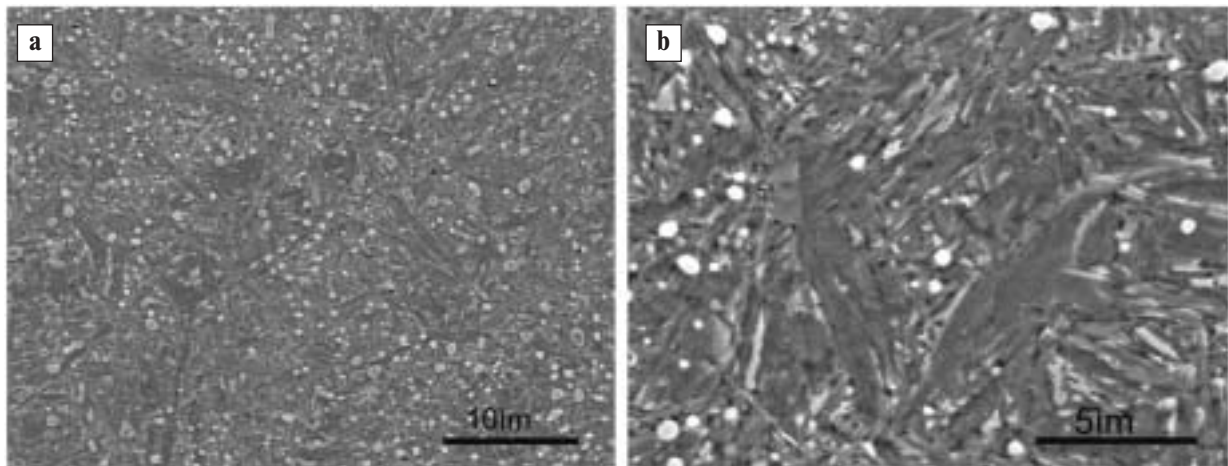


Fig. 2. Microstructure of 14 109 steel. Picric acid etching.

Fractographic analysis revealed that all specimens tested in a high-cycle region failed by fatigue fracture, originating on internal defects of various types. An example of a large aluminium oxide inclusion can be seen in Fig. 4. The inclusion contains nearly 42 % of Al, 53 % O (determined by X-ray diffractometric analysis, wt. %) and the rest is made of Fe, Cr and C. In Fig. 5 an example of a small TiN inclusion is shown. The corresponding composition is 66 % Ti, 19 % N, 9% Cr, and the rest is Fe, V and Zr. The fracture surfaces exhibit typical fish eye appearance with an inclusion at the centre.

4. Discussion

A large scatter of experimental lifetime data in a high-cycle region is a typical feature of high strength bearing steels. This holds not only for a particular batch but it is even more pronounced when experimental results on steels of a similar chemical composition and heat treatment but coming from different steel-makers are compared. The $S-N$ curves cannot be exactly defined. There is no good correlation between the stress amplitude and the number of cycles to fracture, Fig. 3. Results obtained in this work are shown along with high-cycle fatigue data of JIS SUJ2 and NF 106C steel, published in [11] in Fig. 6. It can be concluded that high-cycle lifetime of 14 109 steel fits well into the broad range of results obtained in bearing steels.

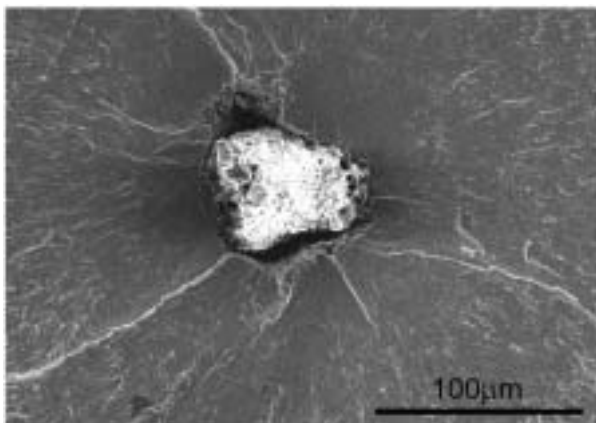


Fig. 4. Large aluminium oxide inclusion at the fatigue crack origin.

In some cases the $S-N$ curves have been interpreted as “two-stage” curves, having a horizontal step in the vicinity of a conventional fatigue limit at an interval of between 10^6 to 10^7 cycles. Experimental results shown in Fig. 3 do not exhibit any sign of a horizontal step. In the frame of the large scatter there seems to be rather a continuous decrease of lifetime following the decrease of stress amplitude. This finding supports suggestion proposed in [6], [11], namely that the $S-N$ curve determined on rotating bending specimens can be influenced by the small size of an extremely loaded volume of material related to large stress gradients in such a way that the $S-N$ curve manifests itself as a step curve.

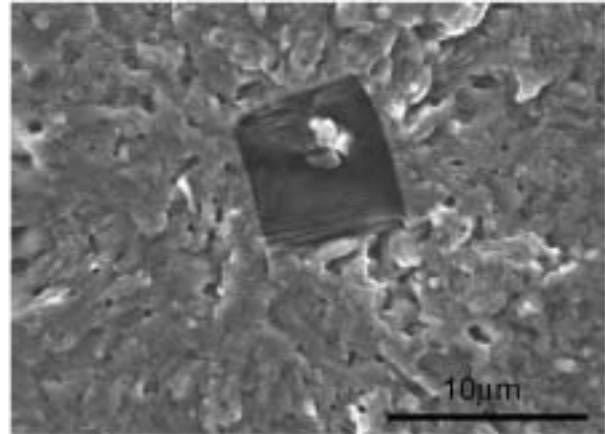


Fig. 5. TiN inclusion in the middle of a fish eye.

Fatigue fracture of bearing steels originate in high-cycle fatigue, mostly at non-metallic inclusions like Al_2O_3 , CaO or SiO_2 . This is in full agreement with fractographic observations, Fig. 4 and 5. All fatigue cracks were initiated at internal inclusions. The influence of small defects or inclusions on fatigue limit can be estimated by an empirical \sqrt{area} method, proposed by Murakami [12]. The \sqrt{area} parameter is defined as the square root of the projected area of a defect into the plane perpendicular to the loading direction. The fatigue limit for symmetrical loading σ_w of a specimen with an internal defect that can be characterized by the geometrical parameter \sqrt{area} can be predicted according to the formula

$$\sigma_w = 1.56(HV + 120)(\sqrt{area})^{-1/6}. \quad (1)$$

HV stands for Vicker's hardness, \sqrt{area} is in μm , and fatigue limit is in MPa. Fractographic observation made it possible to detect and evaluate dimensions of inclusions located in the origin of fatigue fracture almost for all tested specimens. The inclusion dimensions represented \sqrt{area} by parameter, the number of cycles to fracture N_f and the fatigue limit σ_w , as predicted according to formula (1) taking into account hardness value $HV = 650$, are given in Tab. 2.

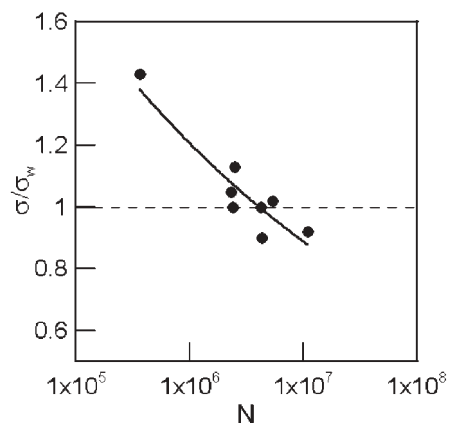


Fig. 7. Modified $S-N$ curve.

Fatigue lifetime, inclusion size at initiation site, and fatigue limit as predicted by $\sqrt{\text{area}}$ of method.

Tab. 2.

σ_a [MPa]	N_f [cycle]	$\sqrt{\text{area}}$ μm	σ_w [MPa]	σ_c/σ_w
900	1.00×10^6	—	—	—
880	2.48×10^6	13.5	778	1.13
880	4.00×10^6	—	—	—
860	3.64×10^5	63.6	601	1.43
860	4.34×10^6	4	953	0.90
860	4.23×10^6	7.4	860	1.00
840	5.39×10^6	9.7	823	1.02
840	2.33×10^6	11.5	800	1.05
820	1.11×10^7	6	892	0.92
800	2.41×10^6	11.4	801	1.00

The highest stress amplitude at which the run-out specimens (on the conventional basis of 10^7 cycles) were observed is, according to Fig.3, $\sigma_c = 840$ MPa. Fig. 7 shows the modified $S-N$ curve

according to Murakami [4]. It can be seen, that the values of σ/σ_w ratio can decrease below 1. This supports the opinion that the conventional number of cycles of the order of 10^7 is insufficient for reliable determination of the fatigue limit of bearing steels [11], where the mechanism of fatigue initiation is related to the role of internal inclusions.

5. Conclusions

The $S-N$ curve of 14 109 bearing steel determined in tension-compression does not exhibit a two-stage form. All fatigue cracks in the high-cycle region were initiated at internal inclusions; a considerable scatter of experimental data is related to this fact. Determination of fatigue limit on the basis of 10^7 is insufficient for this steel; a higher number of cycles has to be used.

Acknowledgements

This work was supported by The Centre for Transportation Research (CETRA, Žilina), the project of bilateral Czech-Slovak co-operation Nr. 36 and the grant No. 1/1077/04 of the Scientific Grant Agency of Ministry of Education and Slovak Academy of Sciences, Slovak Republic.

References

- [1] BENGA, G. C., ABRAO, A. M.: *Turning of hardened 100Cr6 bearing steel with ceramic and PCBN cutting tools*. Journal of Mat. Processing Technol., 143-144 (2003) 237-241.
- [2] MOYER, C.: *Fatigue life prediction of bearings*. In: *Fatigue and Fracture*, ASM Handbook, Vol.19. ASM Int. Materials Park, OH, 1996, p.355-368.
- [3] JECH, J.: *Bearing steels and its heat treatment (in Czech)*, SNTL Praha 1968.
- [4] MURAKAMI, Y., NOMOTO, T., UEDA, T.: *Factors influencing the mechanism of superlong fatigue failure in steels*. Fatigue Fract Engng Mater Struct 22 (1999) 581-590.
- [5] MUGHRABI, H.: *On the life-controlling microstructural fatigue mechanisms in ductile metals and alloys in the gigacycle region*. Fatigue Fract Engng Mater Struct. 22 (1999) 633-641.
- [6] MURAKAMI, Y., YOKOYAMA, N. N., NAGATA, J.: *Mechanism of fatigue failure in ultralong life regime*. Fatigue Fract Engng Mater Struct 25 (2002) 735-746.
- [7] SAKAI, T., SATO, Y., OGUMA, N.: *Characteristic S-N properties of high-carbon-chromium-bearing steel under axial loading in long-life fatigue*. Fatigue Fract Engng Mater Struct 25 (2002) 765-773.
- [8] TANAKA, K., AKINIVA, Y.: *Fatigue crack propagation behaviour from S-N data in very high cycle region*. Fatigue Fract Engng Mater Struct 25 (2002) 813-822.
- [9] SHIOZAWA, K., LU, L.: *Very-high cycle fatigue behaviour of shot-peened high-chromium bearing steel*. Fatigue Fract Engng Mater Struct 25 (2002) 775-784.
- [10] WANG, Q. Y., BATHIAS, C., KAWAGOISHI, N., CHEN, Q.: *Effect of inclusion on subsurface crack initiation and gigacycle fatigue strength*. Int. J. Fatigue 24 (2002) 1269-1274.
- [11] MARINES, I., DOMINGUEZ, G., BAUDRY, G., VITTORI, J.-F., RATHERY, S., DOUCET, J.-P., BATHAIS, C.: *Ultrasonic fatigue tests on bearing steel AISI-SAE 52100 at frequency of 20 and 30 kHz*. Int. J. Fatigue 25 (2003) 1037-1046.
- [12] MURAKAMI, Y., ENDO, M.: *Effects of defects, inclusions and inhomogeneities on fatigue strength*. Int. J. Fatigue 16 (1994) 163 - 182.